ORIGINAL ARTICLE

Synthesis of magnetic Fe_3O_4/activated carbon prepared from banana peel (BPAC@Fe_3O_4) and salvia seed (SSAC@Fe_3O_4) and applications in the adsorption of Basic Blue 41 textile dye from aqueous solutions

Aynaz Mohammadifard[1] · Dalia Allouss[2] · Mehdi Vosoughi[3,4] · Abdollah Dargahi[3] · Amir Moharrami[1]

Abstract

Textile industries use large amounts of water and chemicals for finishing and dying processes. The chemical structures of dyes vary enormously, and some have complicated aromatic structures that resist degradation in conventional wastewater treatment processes because of their stability to sunlight, oxidizing agents, and microorganisms. The objective of this research is to compare the adsorption efficiency of two types of magnetic activated carbons derived from Banana peel and Salvia seed for the removal of basic blue 41 dye. The faculty of the produced activated carbons to remove basic blue 41 dye from aqueous solutions via batch adsorption has been examined under several operating conditions such as pH, adsorbent dose, initial adsorbate concentration and contact time. The cheap, non-toxic produced activated carbons (AC) were characterized by scanning electron microscope and Brunauer-Emmett-Teller analyses. The best conditions of dye adsorption with BPAC@ Fe_3O_4 equal to pH = 9, AC dose 0.5 g/L, dye concentration 50 mg/L and equilibrium contact time 30 min, optimal dye adsorption conditions for SSAC@Fe_3O_4 equal to pH = 9, adsorbent dose 0.75 mg/L, dye concentration 50 mg/L and equilibrium contact time is 30 min. This study followed the Langmuir isotherm model well with regression coefficient of R^2 = 0.9886 for BPAC@Fe_3O_4 and regression coefficient of R^2 = 0.9764 for SSAC@Fe_3O_4.

Keywords Basic blue 41 dye · Activated carbon · Banana peel and salvia seed · BPAC@Fe_3O_4 and SSAC@Fe_3O_4 · Adsorption

Introduction

Textile industry wastewater contains various types of pollutants such as dyes, chemical oxygen demand (COD), biochemical oxygen demand (BOD) and other toxic resistant compounds that are discharged into the environment, especially the receiving waters with irreversible health and environmental hazards (Hasani et al. 2021; Peyghami et al. 2021). Contamination of this wastewater in proportion to the colors in the wastewater reduces the penetration of light into the receiving water. The numerical value of the BOD/COD ratio indicates the degree of biodegradability of organic matter, which in the case of colored wastewater is usually less than 0.25, and indicates that such wastewater contains a large amount of biodegradable organic matter (Chiou et al. 2006; Samarghandi et al. 2021; Dargahi et al. 2021b; Azizi et al. 2019). The dyes used in the textile industry are divided into several groups: 1- Anionic dyes (acidic, direct and reactive), 2- Cationic dyes (all base dyes), 3- Non-dye dyes (Karadag et al. 2007). Basic blue 41 dye with molecular formula $C_{20}H_{26}N_4O_6S$, color index number 11105, molecular weight 450 g/mol, and wavelength 600 nm can be seen in industrial wastewater (Fig. 1) (Mahmoudi et al. 2007).

Colored wastewater treatment methods are classified into three groups: physical methods and chemical and

✉ Mehdi Vosoughi
mvn_20@yahoo.com

✉ Abdollah Dargahi
a.dargahi29@yahoo.com

1 School of Health, Ardabil University of Medical Sciences, Ardabil, Iran

2 Laboratoire de Matériaux, Catalyse et Valorisation des Ressources Naturelles, URAC 24, FST, Université Hassan II-Casablanca, Casablanca, Morocco

3 Social Determinants of Health Research Center, Ardabil University of Medical Sciences, Ardabil, Iran

4 Department of Environmental Health Engineering, School of Public Health, Ardabil University of Medical Sciences, Ardabil, Iran
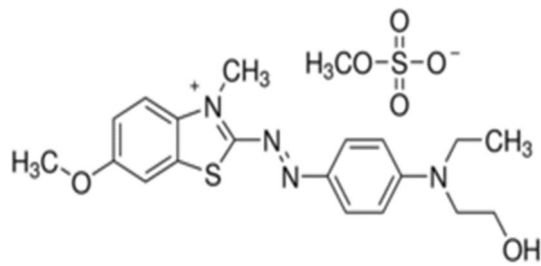
Fig. 1 Structural formula of BB41 dye

biological processes, Among these methods, adsorption on activated carbon, sedimentation, chemical oxidation, optical and biological decomposition and coagulation are common (Malakootian and Moridi 2017; Samarghandi et al. 2020a; Pirsaheb et al. 2016). Among the common removal methods, adsorption is recognized as a promising technique due to its simplicity, low cost and high efficiency (Zhong et al. 2012; Samarghandi et al. 2020b). Zeolites, alginates, chitosans, clays, etc. have been suggested as adsorbents. Activated carbon is the most widely used adsorbent today due to its wide surface area, porosity and high adsorption capacity (Lim et al. 2009). The efficiency of the adsorption process using commercial activated carbon to remove various dyes from the effluent has made it an ideal method compared to other expensive treatment technologies (Temdrara et al. 2013; Samarghandi et al. 2021a). Agricultural products and by-products are abundant and necessarily disposable waste, when they are disposed of by incineration, they produce CO_2 and other forms of pollution. Production of activated carbon from horticultural waste, in addition to cheap production of this product and meeting many industrial and environmental needs, also reduces the volume of production waste (Sayyahzadeh et al. 2012; Shokoohi et al. 2018). Salvia seeds due to their fatty acid groups and banana peel also have a very high amount of carbon in their composition due to their carbohydrate groups and can be used in the production of activated carbon (Razavi et al. 2013; Zazouli and Balarak 2016). Magnetic activated carbon has a unique property so that magnetic nanoparticles coated with activated carbon can be easily separated by an external magnetic field (Shokoohi et al. 2020). Unfortunately, the main problem with using powdered activated carbon or adsorbents with nanosize or nanoparticles is their separation from the solution due to the small particle size, so dispersion and secondary contamination are the main problems of these systems. Therefore, magnetizing these adsorbents can be a suitable solution to solve many of these problems. Recently, the magnetic separation method has been widely used due to its low cost, simplicity and

optimal speed as well as high efficiency (Salehnia et al. 2016; Kakavandi et al. 2014).

In the present study, the efficiency of magnetic activated carbon of banana peel (BPAC@Fe$_3$O$_4$) and magnetic activated carbon of Salvia seed (SSAC@Fe$_3$O$_4$) in the removal of cationic dye BB41 were compare.

Materials and methods

Materials

The dye stock solution was prepared by dissolving the dye powder in double distilled water. Raw materials including BB41 dye powder from Alvan Sabet Hamedan Company and iron (II) chloride, iron (III) chloride, 25% ammonium, phosphoric acid, sulfuric acid, sodium hydroxide were prepared from Merck company in Germany. H_2SO_4 and NaOH In order to adjust the pH of the solution containing dye and for reading and calculating the dye concentration, spectrophotometric device model DR-5000 made in Germany was used. All these experiments were performed on a laboratory scale in the chemistry laboratory of the Faculty of Health of Ardabil University of Medical Sciences.

Synthesis of Fe$_3$O$_4$ nanoparticles

Fe$_3$O$_4$ nanoparticles with a weight ratio of two to one were synthesized by chemical co-precipitation method (Ozmen et al. 2010). In this method, 5.4 g of iron (II) chloride and 2.78 g of iron (III) chloride in a volume of 250 mL of distilled water were dispersed using ultrasonication. Homogenization was performed at 70 °C by adding 20 mL of ammonia solution dropwise until the pH of the solution reached 9. At a pH of about 9, a black precipitate containing magnetic nanoparticles formed. The formed precipitate was stirred for 45 min. It was then rinsed several times with double distilled water to remove impurities. Finally, using 1.3 Tesla magnet, the magnetized Fe$_3$O$_4$ nanoparticles were separated and dried in an oven at 70 °C for 12 hr and then in containers (Ozmen et al. 2010).

Activated carbon production

Dried banana peel and dried salvia seeds were used to prepare activated carbon. To prepare each type of activated carbon, 200 gr of finely chopped banana peel and chopped salvia seeds were first soaked in concentrated phosphoric acid for 24 h. The acid-impregnated wood was transferred to a steel reactor and placed in an electric furnace with temperature and time adjustment at 650 °C for 2 h. After cooling the electric furnace, the reactor contents were washed several times with distilled water by vacuum filter to reach

a near neutral pH. Finally, the activated carbon in the oven was dried at 110 °C for 24 h and after cooling inside the desiccator, it was pulverized by hand mortar and stored in a closed container(Mahvi and Heibati 2010).

Synthesis of AC@Fe$_3$O$_4$ nanocomposites

After the synthesis of Fe$_3$O$_4$ nanoparticles, the loading process was performed by conventional immersion method on activated carbon. For this purpose, 8 g of activated carbon was added to a solution of Fe$_3$O$_4$ nanoparticles with a specific weight, which was equivalent to 20% by weight of iron oxide in the final product, and was mixed vigorously for 3 h. After immersion process, the resulting nanocomposite was dried in an oven at 110 °C for 12 h (Pourfayaz et al. 2016).

BB41 dye adsorption experiments

Stoke solution of 1000 mg/L BB41 dye was used for adsorption experiments. In this research, the variables of pH (3, 5, 7, 9), contact time (5-10-15-20-30-60 min), adsorbent dose (0.25, 0.5, 0.75, 1.0 g/L) and initial concentration of BB41 dye (25, 50, 75, 100 mg/L) were considered as effective parameters in the process of adsorption of BB41 dye. Normal sulfuric acid and sodium hydroxide were adjusted and a certain amount of AC@Fe$_3$O$_4$ nanocomposite obtained from banana peel and salvia seed was added to the solution and entered the adsorption process. During the process, the solution was stirred by a magnetic stirrer at 250 rpm. Finally, after the contact time had elapsed, the adsorbent was separated using a 1.3 Tesla magnet and prepared to measure the concentration of residual dye. Residual dye concentration

was determined by spectrophotometer. The efficiency and adsorption capacity of the adsorbent were calculated using Equations (1) and (2) (Samarghandi et al. 2021b; Afshin et al. 2021).

$$\left(\frac{(C_O - C_e)}{C_O}\right) \times 100 \tag{1}$$

$$q_e = \frac{[(C_O - C_e) \times V]}{M} \tag{2}$$

where C_0 represents the initial dye concentration and Ce the dye concentration of BB41 after contact with the adsorbent in terms of (mg/L) V volume of solution in terms of (L), M the dry weight of the adsorbent (g), q_e the equilibrium adsorption rate (mg/g) (Moussavi and Emamjomeh 2014)

Results and discussion

Characterization of adsorbents

Scanning electron microscopy (SEM) analysis was performed to evaluate the morphological characteristics of the adsorbent. According to Figs. 2 and 3, which shows the morphological characteristics of the adsorbents used for adsorption processes using scanning electron microscopy (SEM), both adsorbents had large pores and had an almost uniform surface, but the pores and porosity of the adsorbent BPAC@ Fe$_3$O$_4$ was higher than SSAC@Fe$_3$O$_4$ and also corresponded to the level of activated carbon used in the study entitled
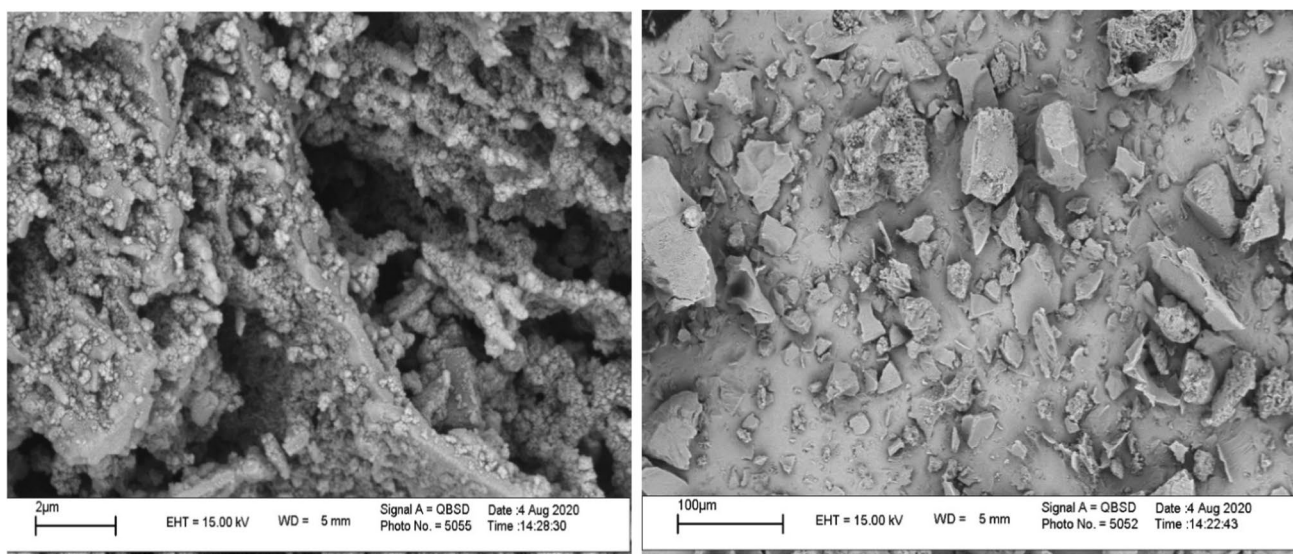
Fig. 2 Scanning electron micrographs (SEM) of PBAC@Fe$_3$O$_4$
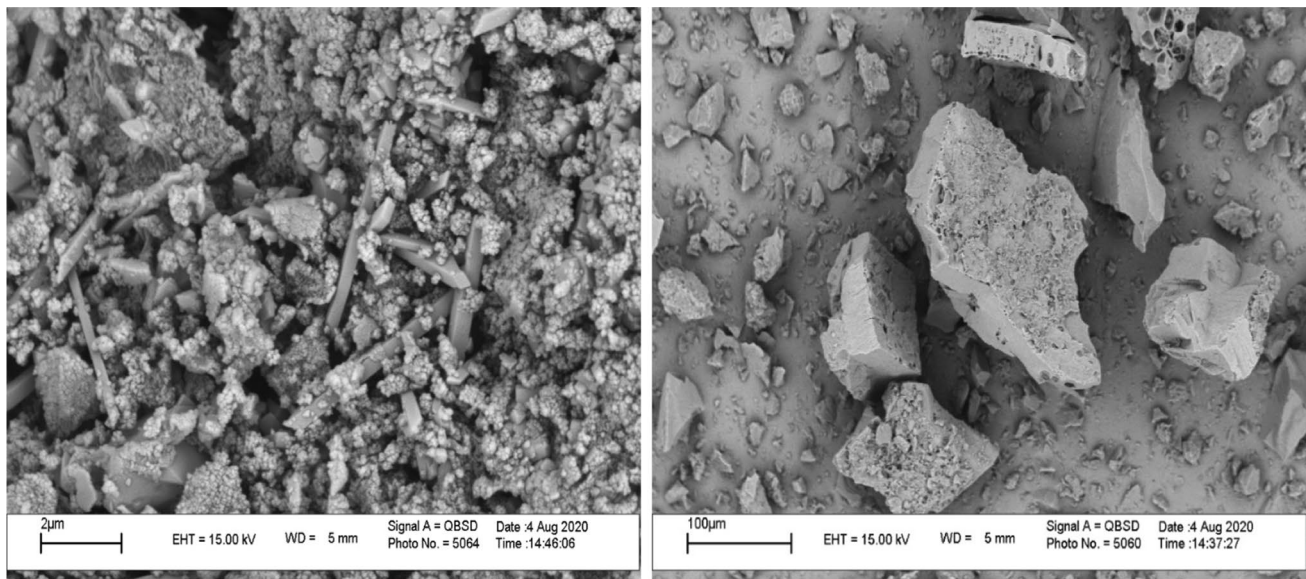
Fig. 3 Scanning electron micrographs (SEM) of SSAC@Fe$_3$O$_4$

Table 1 BET analysis data for the adsorbent investigated in this study

BET test	Adsorbent used	
	BPAC@Fe$_3$O$_4$	SSAC@Fe$_3$O$_4$
Total pore volume	0.6497 cm^{3}g^{-1}	0.2767 cm^{3}g^{-1}
Special adsorbent surface	394.85 cm^{2}g^{-1}	160.02 cm^{2}g^{-1}
The volume required to form a monolayer gas	90.718 (cm^3(STP) g^{-1})	36.766 (cm^3(STP)g^{-1})
Average pore diameter	6.5813 nm	6.9169 nm

"Dynamic Isotherms in Activated Carbon" conducted by Mata et al (Matta et al. 2008).

In order to measure the porosity and specific surface area of adsorbents, Brunauer-Emmett-Teller (BET) was used, which is very effective in studies related to the adsorption of pollutants (Rashidi and Yusup 2017). Table 1 and Fig. 3 show the results of BET analysis for magnetic activated carbon obtained from banana peel and salvia seed. According to this diagram, the specific surface area BPAC@Fe$_3$O$_4$ and SSAC@Fe$_3$O$_4$ are 394.85cm2/g and 160.02 cm^2/g, respectively. According to Table 1 and Fig. 4, the total pore volume and the area of the specific adsorbent surface BPAC@Fe$_3$O$_4$ is more than 2 times SSAC@Fe$_3$O$_4$, which indicates a higher degree of porosity BPAC@Fe$_3$O$_4$, so banana peel can be used as a promising raw material for activated carbon production. The results shown were consistent with a study of the effect of banana peel activated carbon on the removal of methylene blue and orange 2 by Ma et al (Ma et al. 2015).

Parametric study of the adsorption of BB41

Effect of solution pH

BB41 dye is unstable under alkaline dyeing conditions and weakens due to chromophore degradation, but under acidic conditions dye stabilization on synthetic fibers is more effective (Humelnicu et al. 2017). Control of the pH parameter is so important in the adsorption process that it affects both the molecular structure of the dye and the chemical properties of the activated carbon, such as surface charge and the separation of functional groups (Olgun and Atar 2009). Figure 5 shows the effect of the pH of the solution on the reaction. It is observed that with increasing pH, the contaminant removal efficiency by both adsorbents increases. In BPAC@Fe$_3$O$_4$ between intervals 3 to 5 and in SSAC@Fe$_3$O$_4$ between intervals 5 and 7, the highest jump is observed in the color removal process diagram and the highest removal efficiency is observed at pH 9 for BPAC@Fe$_3$O$_4$ and SSAC@Fe$_3$O$_4$ was equal to 61.9% and 49.01%, respectively, so pH = 9 was selected as the optimal pH . According to the diagram in Fig. 5, it is observed that with increasing pH, the adsorption efficiency for both adsorbents increases. Negative charge play The level of activated carbon increases with increasing pH and causes a strong electrostatic bond in cationic dyes (Ahmaditabar et al. 2015; Boudechiche et al. 2019). In the study of Boudechiche et al. 2019. In 2019, the optimal pH of dye adsorption of BB41 using activated carbon obtained from ziziphus lotus was pH = 8 (Boudechiche et al. 2019).
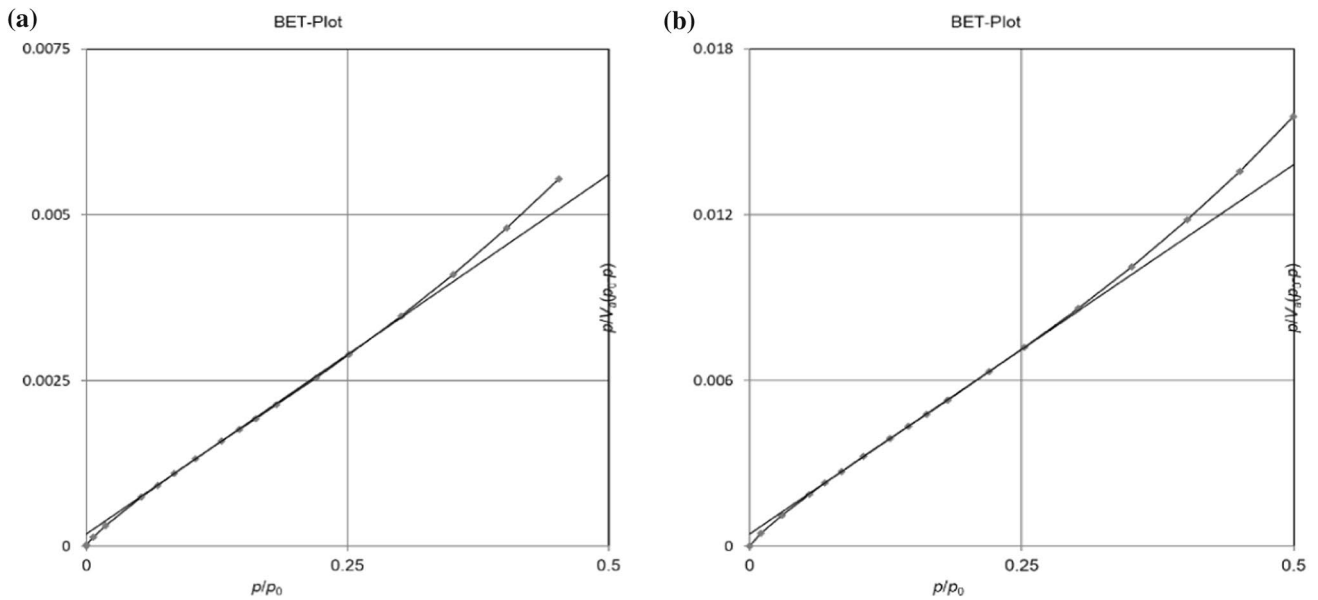
(a)

(b)

Fig. 4 Analysis (BET): **a** BPAC@Fe$_3$O$_4$ and **b** SSAC@Fe$_3$O$_4$
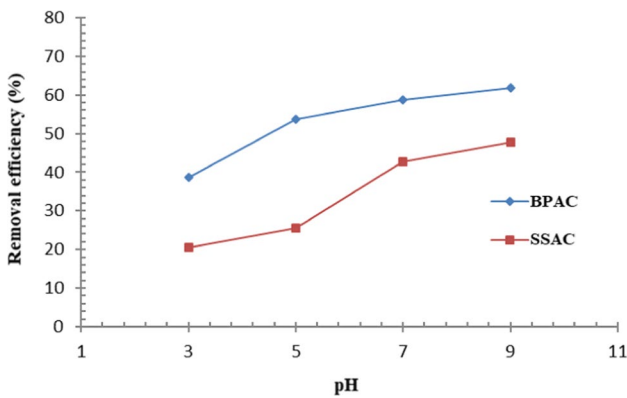
Fig. 5 The effect of pH parameter on the dye removal efficiency of BB41

Effect of adsorbent dose

Figure 6 shows the effect of increasing the adsorbent dose on the amount of dye adsorption by (SSAC@Fe$_3$O$_4$) and (BPAC@Fe$_3$O$_4$) which with increasing the amount of adsorbent increases the removal efficiency and decreases the adsorption capacity. According to the diagram of Fig. 6, a range of (0.1–1 mg/L) was considered for both adsorbents. The slope of the contaminant removal process for both adsorbents is ascending to the dose of 0.75 mg/L and then equilibrium. Therefore, at the dose of 0.75 mg/L, the removal efficiencies for (BPAC) and (SSAC) were 97.22% and 88.16%, respectively, and were selected as the optimal dose for both adsorbents. According to the diagram in

Fig. 6 The effect of the amount of adsorbent on the dye removal efficiency of BB41

Fig. 6, the increase in the adsorbent dose increases due to the increase in the number of sites available for adsorption efficiency, but because the dye concentration is constant at high doses, the existing sites remain unsaturated, which led to a decrease in the amount of dye adsorbed per unit mass of adsorbent. The results of the study by Fil et al. 2013 are similar to this study (Ahmadabadi et al. 2016; Fil et al. 2013). Table 4 shows a comparison of the adsorption capacity of different adsorbents in BB41 dye removal. According to Table 2, it can be seen that BPAC and SSAC adsorbents have a very high adsorption capacity compared to the adsorbents used in previous studies (Afshin et al. 2018).

Effect of time and initial concentration of dyes

As shown in Fig. 6, in the reaction of both adsorbents, the removal efficiency decreases with increasing concentration of contaminants, and also with increasing contact time, the removal efficiency increases, and in 30 min, both reactions reach equilibrium. The studied system was performed by
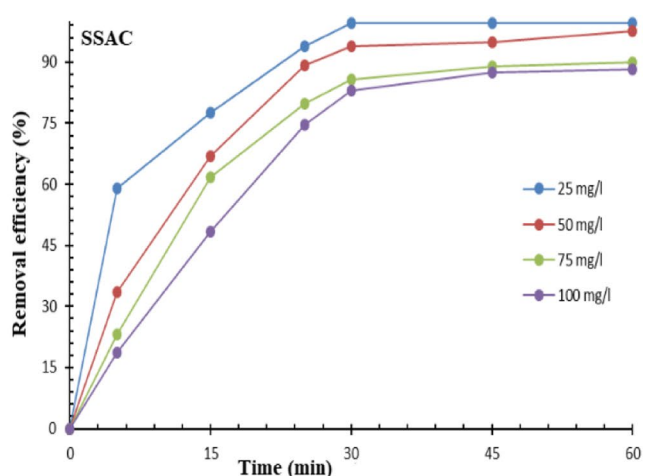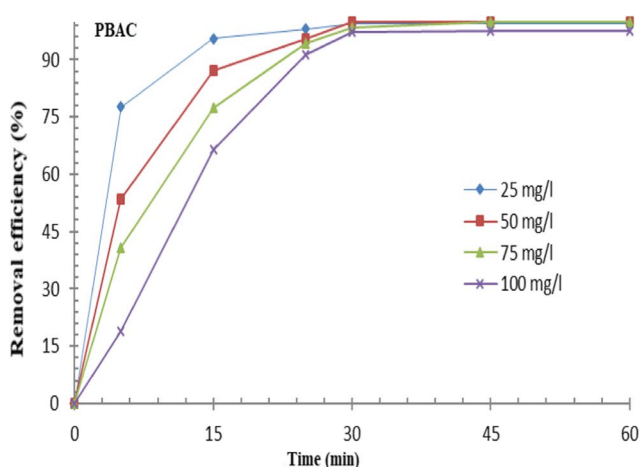
changing the initial concentration of contaminants (25-25 mg/L). According to Fig. 6 in contact time of 30 min, the highest dye removal efficiencies by BPSAC@Fe_3O_4 and SSAC@Fe_3O_4 were 97.79% and 98.23%, respectively. As can be seen in Fig. 6, with increasing BB41dye concentration, the adsorption efficiency decreased due to the fact that at a constant amount of absorbent dose, the active sites of adsorption are constant; however, with increasing the concentration of adsorbent, the number of contaminants in the reaction medium increases, so the removal efficiency decreases (Alidadi et al. 2017). This may also indicate that the equilibrium time does not change with the initial concentration of BB41 dye (Kooli et al. 2015). Due to the increase in time, the removal efficiency increases and reaches equilibrium at different concentrations but at the same time, i.e., 30 min. In other words, at this moment, the amount of adsorbed dye reaches the dynamic equilibrium with the amount of desorbed dye (Ahmad and Alrozi 2011; Acharya et al. 2009; MORADI NASAB et al. 2016) (Fig. 7).

Adsorption isotherms

Isothermal equations with Langmuir and Freundlich models were used to evaluate the experimental data and describe the equilibrium state between solid phase (AC@Fe_3O_4 nanocomposite) and liquid (dye solution). The Langmuir isotherm model represents the uniform and a layer adsorption of adsorbent material with the same energy on all adsorbent surfaces. While Freundlich equation is based on multilayer, non-uniform and heterogeneous adsorption of adsorbent on adsorbent. The linear form of the Langmuir and Freundlich isotherm equations is presented in Equations (3) and (4) (Afshin et al. 2019):

Table 2 Comparison of adsorption capacity of different adsorbents in BB41 dye removal

Adsorbent	q_m (mg/g)	References
Sodium alginate	12	Mahmoodi et al. (2012)
Raw rice husk	24.4	Karaj (2016)
Modified rice husk	34.6	Karaj (2016)
Untreated antibiotic waste	111	Yeddou-Mezenner (2010)
N, F-codoped flower-like TiO$_2$	143	Jiang et al. (2013)
Alga activated carbon	125	Afshin et al. (2018)
BPAC	333.33	This study
SSAC	303.03	This study

Fig. 7 The effect of time and concentration of BB41 on adsorption by PBAC and SSAC

$$\frac{1}{q_e} = \frac{1}{k_L q_m c_e} + \frac{1}{q_m} \qquad (3)$$

In these equations, C_e is the equilibrium concentration of BB41 in terms of (mg/L), q_e is the amount of dye adsorbed per unit mass of adsorbent (mg/g), q_m represents the maximum adsorption capacity in terms of (mg/g), and the Langmuir constant K_L is (L/mg).

$$\log q_e = \log k_f + \frac{1}{n} \log c_e \qquad (4)$$

K_f and n are Freundlich constants and depend on the adsorption capacity and intensity. If the values of n are less than one, they indicate poor adsorption and the values of 1–2 and 2–10 also indicate moderate and desirable adsorption, respectively. In the Langmuir equation, the type of utility can also be determined using factor values without the R_L dimension (Eq. 5) (Rashtbari et al. 2020).

$$R_L = \frac{1}{1 + K_L C_0} \qquad (5)$$

If the value of $1 < R_L$ shows undesirable adsorption, $R_L = 1$ shows linear adsorption, $R_L = 0$ indicates irreversible adsorption and $1 < R_L < 0$ shows optimal adsorption (Samarghandi et al. 2019a, b; Dargahi et al. 2021; Alizadeh et al. 2017).

Since the optimal contact time for both adsorbents is 30 min, so for 30 min, a pH of 9 was prepared to investigate the adsorption isotherm. Figure 8 shows the Langmuir model isotherm diagram and Fig. 9 shows the Freundlich model isotherm diagram. The maximum adsorption capacity is shown. In the Langmuir isotherm model for BPAC@ Fe_3O_4 and SSAC@Fe_3O_4, it is equal to 333.33 and 303.03, respectively. According to Table 3, the best isotherm for both adsorbents is the Langmuir isotherm. As can be seen from the results of Figs. 8 and 9, Table 3, dye adsorption using AC @Fe3O4 nanocomposite in the present study with regression coefficient of 0.9886 for BPAC@Fe_3O_4 and regression coefficient of 0.964 for SSAC@Fe_3O_4 follows the Langmuir
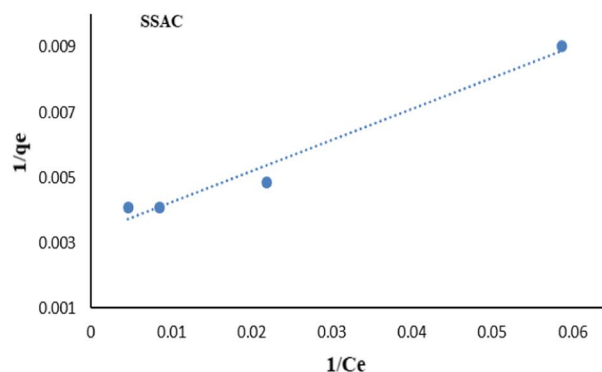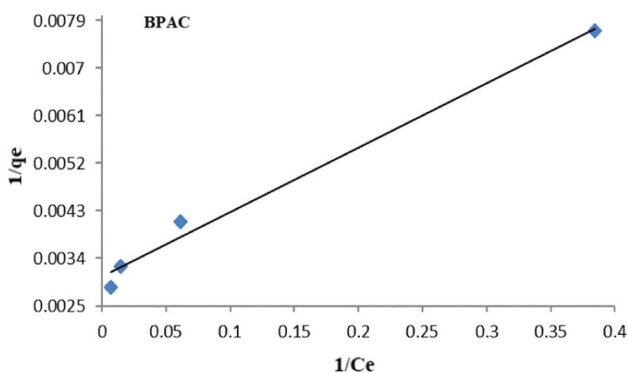

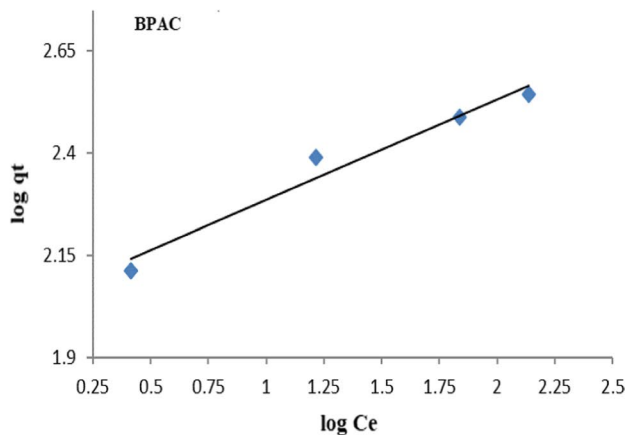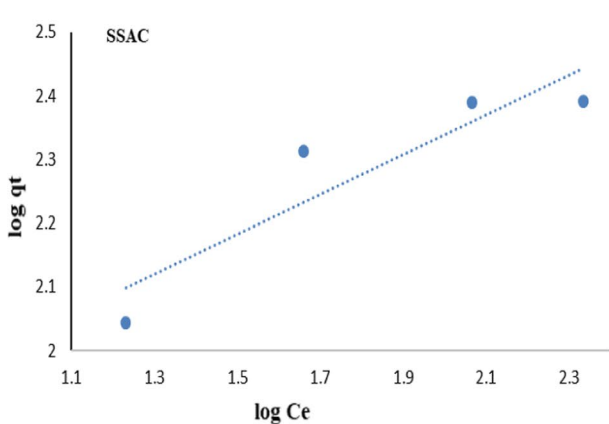Fig. 8 Langmuir isotherm models of adsorption BB41 by PBAC and SSAC

Fig. 9 Freundlich isotherm models of adsorption BB41 by PBAC and SSAC

Table 3 Adsorption isotherm data for the removal of BB41 dye by adsorption process

| Adsorption isotherms	Langmuir isotherm model				Freundlich isotherm model		
	R_L	R^2	K_l (L/mg)	q_m (mg/g)	Kf [(mg/g) (mg/L)1/n]	n	R^2
BPAC@Fe$_3$O$_4$	0.40	0.9886	0.2459	33.333	109.22	4.06	0.9649
SSAC@Fe$_3$O$_4$	0.22	0.9746	0.346	303.03	51.96	3.21	0.8377

isotherm model. The Langmuir isotherm model is known as the most widely used adsorption isotherm for soluble adsorption of solutions and has often been successfully applied to adsorb a variety of contaminants from water (El Qada et al. 2008). Which is consistent with the results of the study of (Afshin et al. 2018). Also, the results of Ashrafi et al study in 2015 regarding the study of BB41 dye adsorption by NaOH-modified rice husk adsorbent with regression coefficient of 0.9865 were very similar to this study (Ashrafi et al. 2016).

Adsorption kinetics

Adsorption kinetics examines important information to understand the mechanisms of adsorption and to evaluate the performance of adsorbents (Hassani et al. 2014). Kinetic equations are used to describe the transfer behavior of adsorbed material molecules per unit time and to study the reaction rate. In the present study, pseudo-first and pseudo-second kinetic models were used. Equations (6) and (7) (Alipour et al. 2021) show the Pseudo-first and pseudo-second kinetic models, respectively.

$$\log\left(q_e - q_t\right) = \log q_e - \left(\frac{k_1 t}{2.303}\right) \tag{6}$$

$$\frac{t}{q_e} = \frac{1}{(k_2 q_e^2)} + \left(\frac{1}{q_e}\right)t \tag{7}$$
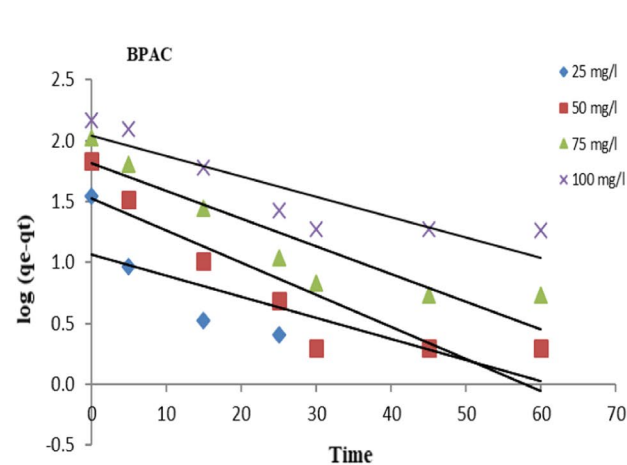
q_e and qt are the adsorption capacities at equilibrium and at time t and k$_1$ (min^{-1}) and k$_2$ the adsorption rate constant in the pseudo-first and pseudo-second kinetic models, respectively (Samarghandi et al. 2019a, b; Dargahi et al. 2021a).

Figure 10 shows in the pseudo-first graphs and Fig. 11 shows pseudo-second kinetic models graphs and Table 4 shows the data of the kinetic equations of the reactions. Pseudo-first and pseudo-second equations of kinetic models were obtained at different concentrations in the range 25–100 mg/L. According to Table 4 at a concentration of 25 mg/L, the regression coefficient of pseudo-first and pseudo-second equations for magnetic activated carbon obtained from banana peel 0.628 and 0.995, respectively, and for activated carbon obtained from salvia seed equal to 0.7842 and 0.994. According to Table 4 and the diagrams in Figs. 10 and 11, both magnetic activated carbon (BPAC@Fe$_3$O$_4$) and (SSAC@Fe$_3$O$_4$) have $R^2 < 0.95$ in the pseudo -first-order model and $R^2 > 0.95$ in the pseudo-second model (Boudechiche et al. 2019). And follow the pseudo- second kinetic model well, which indicates the quality of the adsorbents used. The results were consistent with the study of (Regti et al. 2017).
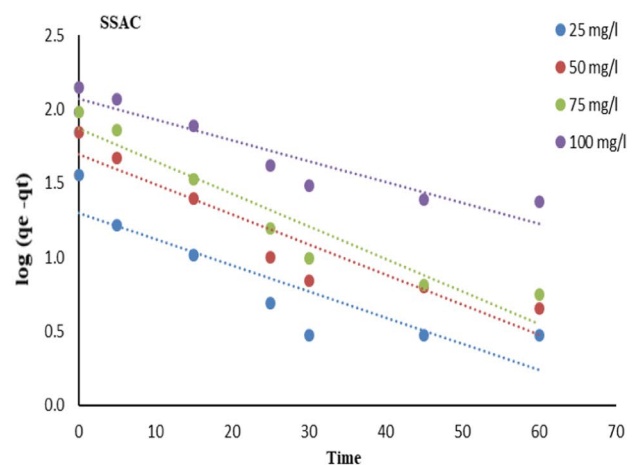
Fig. 10 Pseudo-first kinetic data of adsorption by BPAC and SSAC
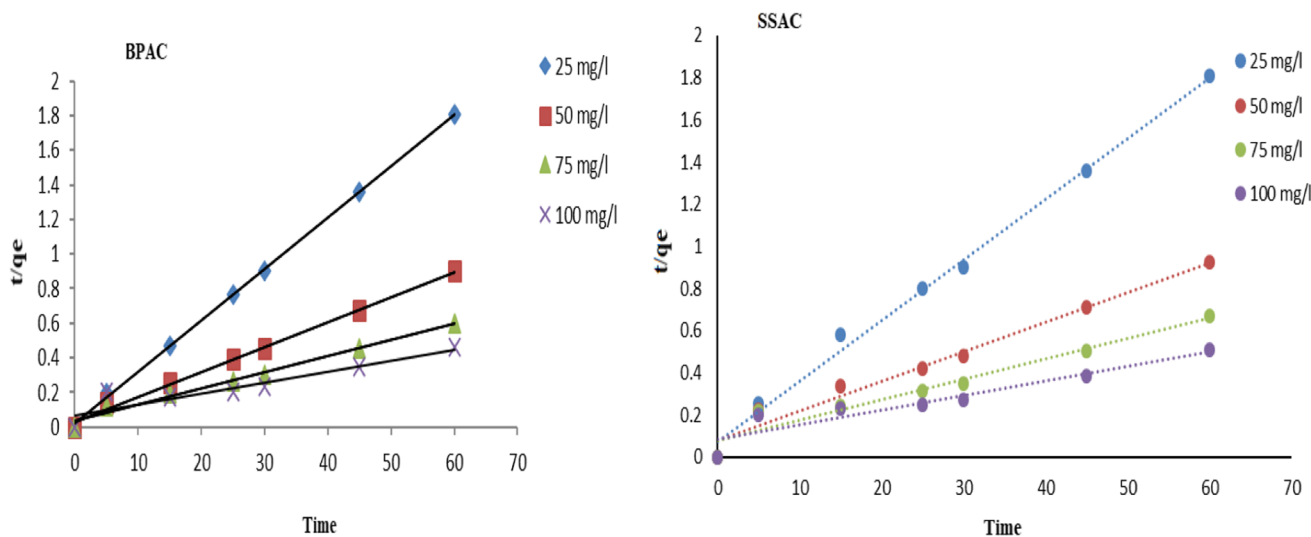
Fig 11 Pseudo-second kinetic data of adsorption by BPAC and SSAC

Table 4 The kinetics of adsorption reactions for the removal of BB41 dye by adsorption process

Dye concentration (mg /l)		Pseudo-first kinetic				Pseudo-second kinetic		
		$q_{e,epx}$ (mg/g)	$q_{1,cal}$ (mg/g)	k_1 (1/min)	R^2_1	$q_{2,cal}$ (mg/g)	K_2 (g mg/min)	R^2_2
BPAC@Fe$_3$O$_4$	25	35.2	11.73	0.0401	0.628	33.67	0.0426	0.9995
	50	68.5	33.48	0.0606	0.8017	44.69	0.0064	0.9954
	75	105.25	65.09	0.0523	0.8492	107.53	0.0023	0.9861
	100	148.5	99.79	0.0649	0.7974	158.73	0.0006	0.8717
SSAC@Fe$_3$O$_4$	25	36.2	19.96	0.0408	0.7842	34.72	.0.0114	0. 9940
	50	69.5	49.62	0.0407	0.8836	71.43	0.0024	0.9742
	75	95.5	73.42	0.0507	0.9116	103.09	0.0012	0.9450
	100	141.25	118.47	0.0325	0.8872	142.86	0.0005	0.8915

Conclusion

Carbon from agricultural and household wastes can be used to remove emerging pollutants. SEM and BET analyzes for adsorbents used in BB41 dye adsorption experiments showed that the adsorbents have a very high quality due to their large pores and uniform surface as well as having a suitable specific surface area. Adsorption of BB41 dye using magnetic activated carbon prepared from banana peel and salvia seeds, with increasing adsorbent and contact time, adsorption efficiency increases and adsorption capacity also decreases with increasing pH and concentration of BB41 adsorption efficiency decreases. Optimal dye adsorption conditions with BPAC@Fe$_3$O$_4$ equal to pH = 9, adsorbent dose 0.5 g/L, dye concentration 50 mg/L and equilibrium contact time 30 min, optimal dye adsorption conditions for SSAC@Fe$_3$O$_4$ equal to pH = 9, adsorbent dose 0.75 g/L, dye concentration 50 mg/L and equilibrium contact time is 30 min. This study followed the Langmuir isotherm model well with regression coefficient of 0.9886 for BPAC@Fe$_3$O$_4$ and regression coefficient of 0.9764 for SSAC@Fe$_3$O$_4$. Kinetic observations showed that the adsorption behavior of BB41 per unit time followed the pseudo-second kinetic equation. Also, the high adsorption capacity of the adsorbents used in the present study indicates the quality of activated carbon prepared from banana peel and salvia seeds. Therefore, activated carbon can be very useful and efficient in removing pollutants from polluted environments and also its magnetization can be useful in carbon sequestration and not using filters and can be used as an economical and useful method.

Declarations

References

Acharya J, Sahu J, Mohanty C, Meikap B (2009) Removal of lead (II) from wastewater by activated carbon developed from Tamarind wood by zinc chloride activation. Chem Eng J 149(1–3):249–262

Afshin S, Mokhtari SA, Vosoughi M, Sadeghi H, Rashtbari Y (2018) Data of adsorption of basic blue 41 dye from aqueous solutions by activated carbon prepared from filamentous algae. Data brief 21:1008–1013

Afshin S, Rashtbari Y, Shirmardi M, Vosoughi M, Hamzehzadeh A (2019) Adsorption of basic violet 16 dye from aqueous solution onto mucilaginous seeds of salvia sclarea: kinetics and isotherms studies. Desalination Water Treat 161:365–375

Afshin S, Rashtbari Y, Vosough M, Dargahi AF, Behzad MA et al (2021) Application of Box-Behnken design for optimizing parameters of hexavalent chromium removal from aqueous solutions using Fe3O4 loaded on activated carbon prepared from alga: kinetics and equilibrium study. J Water Process Eng 42:102113

Ahmad MA, Alrozi R (2011) Removal of malachite green dye from aqueous solution using rambutan peel-based activated carbon: equilibrium, kinetic and thermodynamic studies. Chem Eng J 171(2):510–516

Ahmadabadi M, Rahdar S, Taghavi M (2016) Evaluation of basic red 18 removals from aqueous solution using peanut shell ash. J Torbat Heydariyeh Univ Med Sci 4(2):21–31

Ahmaditabar A, Dehghani MH, Izadpanah F (2015) Removal of basic violet 16 dye from aqueous solutions by using chitosan extracted from shrimp shells. J Res Environ Health 1(3):186–192. https://doi.org/10.22038/jreh.2015.6181

Alidadi H, Dolatabadi M, Mehrabpour M, Dehghan A (2017) The efficacy of ciprofloxacin removal by chitosan/zeolite composite from aqueous solution: response surface methodology, kinetic and isotherm studies. J Health Field 5:1–12

Alipour M, Vosoughi M, Mokhtari SA, Sadeghi H, Rashtbari Y, Shirmardi M et al (2021) Optimising the basic violet 16 adsorption from aqueous solutions by magnetic graphene oxide using the response surface model based on the Box-Behnken design. Int J Environ Anal Chem 101(6):758–777

Alizadeh B, Delnavaz M, Shakeri A (2017) Treatment of synthetic wastewater containing of CD (II) using novel magnetic EDTA/chitosan/TiO₂ nanocomposite. J Environ Health Eng 4(4):289–298

Ashrafi S, Kamani H, Soheil Arezomand H, Yousefi N, Mahvi A (2016) Optimization and modeling of process variables for adsorption of Basic Blue 41 on NaOH-modified rice husk using response surface methodology. Desalination Water Treat 57(30):14051–14059

Azizi A, Dargahi A, Almasi A (2019) Biological removal of diazinon in a moving bed biofilm reactor–process optimization with central composite design. Toxin Rev 1:11

Boudechiche N, Fares M, Ouyahia S, Yazid H, Trari M, Sadaoui Z (2019) Comparative study on removal of two basic dyes in aqueous medium by adsorption using activated carbon from Ziziphus lotus stones. Microchem J 146:1010–1018

Chiou C-S, Chang C-F, Chang C-T, Shie J-L, Chen Y-H (2006) Mineralization of reactive black 5 in aqueous solution by basic oxygen furnace slag in the presence of hydrogen peroxide. Chemosphere 62(5):788–795

Dargahi A, Hasani K, Mokhtari SA, Vosoughi M, Moradi M, Vaziri Y (2021) Highly effective degradation of 2, 4-Dichlorophenoxyacetic acid herbicide in a three-dimensional sono-electro-Fenton (3D/SEF) system using powder activated carbon (PAC)/Fe₃O₄ as magnetic particle electrode. J Environ Chem Eng 9(5):105889

Dargahi A, Shokoohi R, Asgari G, Ansari A, Nematollahi D, Samarghandi MRJRA (2021) Moving-bed biofilm reactor combined with three-dimensional electrochemical pretreatment (MBBR–3DE) for 2, 4-D herbicide treatment: application for real wastewater, improvement of biodegradability. RSC Adv 11(16):9608–9620

Dargahi A, Samarghandi MR, Shabanloo A, Mahmoudi MM, Nasab HZ (2021) Statistical modeling of phenolic compounds adsorption onto low-cost adsorbent prepared from aloe vera leaves wastes using CCD-RSM optimization: effect of parameters, isotherm, and kinetic studies. Biomass Convers Biorefinery. https://doi.org/10.1007/s13399-021-01601-y

El Qada EN, Allen SJ, Walker GM (2008) Adsorption of basic dyes from aqueous solution onto activated carbons. Chem Eng J 135(3):174–184

Fil BA, Karakaş ZK, Boncukcuoğlu R, Yılmaz AE (2013) Removal of cationic dye (basic red 18) from aqueous solution using natural Turkish clay. Glob Nest J 15(4):529–541

Hasani K, Moradi M, Mokhtari SA, Dargahi A, Vosoughi M (2021) Degradation of basic violet 16 dye by electro-activated persulfate process from aqueous solutions and toxicity assessment using microorganisms: determination of by-products, reaction kinetic and optimization using Box-Behnken design. Int J Chem React Eng 19(3):261–275

Hassani A, Vafaei F, Karaca S, Khataee A (2014) Adsorption of a cationic dye from aqueous solution using Turkish lignite: kinetic, isotherm, thermodynamic studies and neural network modeling. J Ind Eng Chem 20(4):2615–2624

Humelnicu I, Băiceanu A, Ignat M-E, Dulman V (2017) The removal of basic blue 41 textile dye from aqueous solution by adsorption onto natural zeolitic tuff: kinetics and thermodynamics. Process Saf Environ Prot 105:274–287

Kakavandi B, Rezaei Kalantary R, Jonidi Jafari A, Esrafily A, Gholizadeh A, Azari A (2014) Efficiency of powder activated carbon magnetized by Fe₃O₄ nanoparticles for amoxicillin removal from

aqueous solutions: equilibrium and kinetic studies of adsorption process. Iran J Health Environ 7(1):34–21

Karadag D, Akgul E, Tok S, Erturk F, Kaya MA, Turan M (2007) Basic and reactive dye removal using natural and modified zeolites. J Chem Eng Data 52(6):2436–2441

Kooli F, Yan L, Al-Faze R, Al-Sehimi A (2015) Removal enhancement of basic blue 41 by brick waste from an aqueous solution. Arab J Chem 8(3):333–342

Lim S-F, Zheng Y-M, Zou S-W, Chen JP (2009) Removal of copper by calcium alginate encapsulated magnetic sorbent. Chem Eng J 152(2–3):509–513

Ma J, Huang D, Zou J, Li L, Kong Y, Komarneni S (2015) Adsorption of methylene blue and orange II pollutants on activated carbon prepared from banana peel. J Porous Mater 22(2):301–311

Mahmoudi N, Arami M, Gharanjig K, Nourmohammadian F (2007) Decolorization and mineralization of basic dye using nanophoto-catalysis: pilot scale study. J Color Sci Technol 1(1):1–6

Mahvi A, Heibati B (2010) Removal efficiency of azo dyes from textile effluent using activated carbon made from walnut wood and determination of isotherms of acid red18. J Health 1(3):7–15

Malakootian M, Moridi A (2017) Efficiency of electro-fenton process in removing acid red 18 dye from aqueous solutions. Process Saf Environ Prot 111:138–147

Matta GKL, Barros MASD, Lambrecht R, SilvaLima EAOC (2008) Dynamic isotherms of dye in activated carbon. Mater Res 11(3):365–369

Moradi NASAB, Belyani S, Behzad S, Tamadon MF (2016) Removal of reactive-dyes from textile plant effluents using polyvinyl alcohol-coated active carbon obtained from sesame seeds. Water Wastewater 27(4):104

Moussavi, SP, Emamjomeh, M (2014) Study of adsorption isotherms and adsorption kinetics of reactive blue 19 dye from aqueous solutions by multi-wall carbon nanotubes. J Shahrekord Univ Med Sci. 16

Olgun A, Atar N (2009) Equilibrium and kinetic adsorption study of basic yellow 28 and basic red 46 by a boron industry waste. J Hazard Mater 161(1):148–156

Ozmen M, Can K, Arslan G, Tor A, Cengeloglu Y, Ersoz M (2010) Adsorption of Cu (II) from aqueous solution by using modified Fe_3O_4 magnetic nanoparticles. Desalination 254(1–3):162–169

Peyghami A, Moharrami A, Rashtbari Y, Afshin S, Vosuoghi M, Dargahi A (2021) Evaluation of the efficiency of magnetized clinopti-tilolite zeolite with Fe_3O_4 nanoparticles on the removal of basic violet 16 (BV16) dye from aqueous solutions. J of Dispers Sci Technol. https://doi.org/10.1080/01932691.2021.1947847

Pirsaheb M, Sharafi K, Karami A, Dargahi A, Ejraei A (2016) Evaluating the performance of inorganic coagulants (poly aluminum chloride, ferrous sulfate, ferric chloride and al minum sulfate) in removing the turbidity from aqueous solutions. Int J Pharm Technol 8(2):13168–13181

Pourfayaz F, Farzan F, Ahmadiaval P, Bitari H (2016) Synthesis Of magnetically separable nanoadsorbents through the incorporation of magnetite nanoparticles in activated carbon. J Pet Res 25(84):186–193

Rashidi NA, Yusup S (2017) Potential of palm kernel shell as activated carbon precursors through single stage activation technique for carbon dioxide adsorption. J Clean Prod 168:474–486

Rashtbari Y, Hazrati S, Azari A, Afshin S, Fazlzadeh M, Vosoughi M (2020) A novel, eco-friendly and green synthesis of PPAC-ZnO and PPAC-nZVI nanocomposite using pomegranate peel: cephalexin adsorption experiments, mechanisms, isotherms and kinetics. Adv Powder Technol 31(4):1612–1623

Razavi SH, Mortazavi SA, Shakeri M, Toosi BS, Asadolahi E (2013) Evaluating the feasibility of producing antimicrobial film based on sodium caseinate and essential oil of Zataria multiflora Boiss. Iran Food Sci Technol Res J 9(3):195–201

Regti A, Laamari MR, Stiriba S-E, El Haddad M (2017) Removal of Basic Blue 41 dyes using Persea Americana-activated carbon prepared by phosphoric acid action. Int J Ind Chem 8(2):187–195

Salehnia S, Barikbin B, Dorri H (2016) The efficiency of magnetic carbon activated by iron oxide nanoparticles in removing of Cu (II) from aqueous solutions. J Birjand Univ Med Sci 23(1):44–55

Samarghandi M, Asgari G, Shokoohi R, Dargahi A, Moradi Golrokhi M, Faraji H et al (2019) Efficiency of saccharomyces cerevisiae in ceftriaxone removal from aquatic environments: kinetic, isotherm of absorption and thermodynamics study. J Health 10(3):270–286

Samarghandi MR, Asgari G, Shokoohi R, Dargahi A, Arabkouhsar A (2019) Removing amoxicillin antibiotic from aqueous solutions by Saccharomyces cerevisiae bioadsorbent: kinetic, thermodynamic and isotherm studies. Desalination Water Treat 152:306–315

Samarghandi MR, Dargahi A, Rahmani A, Shabanloo A, Ansari A, Nematollahi D (2021) Application of a fluidized three-dimensional electrochemical reactor with Ti/SnO2–Sb/β-PbO2 anode and granular activated carbon particles for degradation and mineralization of 2, 4-dichlorophenol: process optimization and degradation pathway. Chemosphere 279:130640

Samarghandi MR, Dargahi A, Shabanloo A, Nasab HZ, Vaziri Y, Ansari A (2020) Electrochemical degradation of methylene blue dye using a graphite doped PbO$_2$ anode: optimization of operational parameters, degradation pathway and improving the biodegradability of textile wastewater. Arab J Chem 13(8):6847–6864

Samarghandi MR, Dargahi A, Zolghadr Nasab H, Ghahramani E, Salehi S (2020) Degradation of azo dye Acid red 14 (AR14) from aqueous solution using H_2O_2/nZVI and $S_2O_8^{2-}$/nZVI processes in the presence of UV irradiation. Water Environ Res 92(8):1173–1183

Samarghandi MR, Ansari A, Dargahi A, Shabanloo A, Nematollahi D, Khazaei M et al (2021) Enhanced electrocatalytic degradation of bisphenol a by graphite/β-PbO$_2$ anode in a three-dimensional electrochemical reactor. J Environ Chem Eng 9(5):106072

Samarghandi MR, Dargahi A, Rahmani A, Shabanloo A, Ansari A, Nematollahi D (2021) Application of a fluidized three-dimensional electrochemical reactor with Ti/SnO$_2$–Sb/β-PbO$_2$ anode and granular activated carbon particles for degradation and mineralization of 2, 4-dichlorophenol: process optimization and degradation pathway. Chemosphere 279:130640

Sayyahzadeh A, Ganjidoust H, Ayati B (2012) Optimization of activated carbon production from almond shell for adsorption of soluble oil contaminants. J Water Wastewater 25(5):93

Shokoohi R, Gillani RA, Mahmoudi MM, Dargahi A (2018) Investigation of the efficiency of heterogeneous fenton-like process using modified magnetic nanoparticles with sodium alginate in removing bisphenol a from aquatic environments: kinetic studies. Desalination Water Treat 101:185–192

Shokoohi R, Dargahi A, Gilan RA, Nasab HZ, Zeynalzadeh D, Mahmoudi MM (2020) Magnetic multi-walled carbon nanotube as effective adsorbent for ciprofloxacin (CIP) removal from aqueous solutions: isotherm and kinetics studies. Int J Chem React Eng. https://doi.org/10.1515/ijcre-2019-0130

Temdrara L, Khelifi A, Addoun A (2013) Study of methylene blue dye adsorption on to activated carbons from olive stones. Int J Chem Mol Nucl Mater Metall Eng 7:722–724

Zazouli MA, Balarak D (2016) Adsorption of 2-chlorophenol on activated carbon prepared from orange and banana husk: equilibrium and kinetic studies. Saf Promot Inj Prev 4(2):117–128

Zhong Z-Y, Yang Q, Li X-M, Luo K, Liu Y, Zeng G-M (2012) Preparation of peanut hull-based activated carbon by microwave-induced phosphoric acid activation and its application in Remazol brilliant blue R adsorption. Ind Crop Prod 37(1):178–185